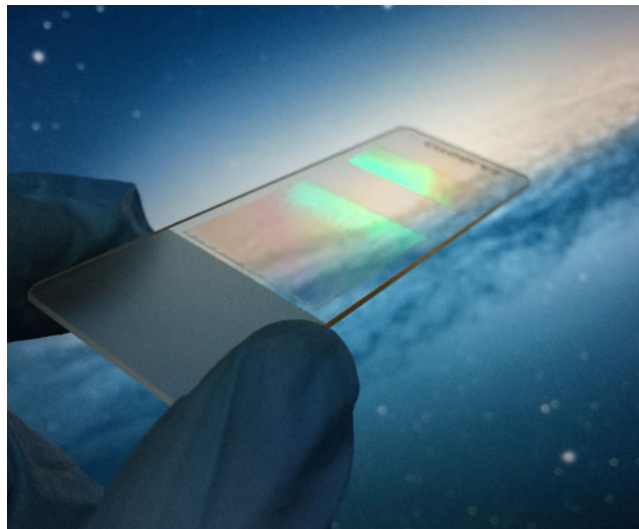


# Diffraction Efficiency Distribution of Output Grating in Holographic Waveguide Display System

Volume 10, Number 04, August 2018

Ao Liu  
Yuning Zhang  
Yishi Weng  
Zhongwen Shen  
Baoping Wang



---

DOI: 10.1109/JPHOT.2018.2856774  
1943-0655 © 2018 IEEE

# Diffraction Efficiency Distribution of Output Grating in Holographic Waveguide Display System

Ao Liu , Yuning Zhang , Yishi Weng, Zhongwen Shen ,  
and Baoping Wang

International Joint Research Laboratory for Information Display and Visualization, School of Electronic Science and Engineering, Southeast University, Nanjing 210096, China

DOI:10.1109/JPHOT.2018.2856774

1943-0655 © 2018 IEEE. Translations and content mining are permitted for academic research only. Personal use is also permitted, but republication/redistribution requires IEEE permission. See [http://www.ieee.org/publications\\_standards/publications/rights/index.html](http://www.ieee.org/publications_standards/publications/rights/index.html) for more information.

Manuscript received July 2, 2018; accepted July 12, 2018. Date of publication July 19, 2018; date of current version July 30, 2018. This work was supported by the National Key Research Program under Grant 2016YFB0401201. Corresponding author: Yuning Zhang (e-mail: zyn@seu.edu.cn).

**Abstract:** Planar waveguide structure has benefits to expand the exit pupil of the near-eye display. To achieve a uniform output luminance within the expanded exit pupil, a specific distribution of diffractive efficiency (DE) should be set for the out-coupling grating. In this paper, a physical model is built to study the DE distribution of out-coupling grating with consideration of the whole field of view. Compared to the previous works, which only considered the central view angle, this model is more consistent with the actual situations to realize a uniform imaging output for a waveguide-based near-eye display system. Also, a planar waveguide with two holographic volume gratings as the in- and out-coupling gratings is fabricated to verify the proposed DE distribution. In experiments, a spatial light modulator is applied as the spatial luminance modulator, and the coupling grating with the proposed DE distribution is fabricated by the holographic interference exposure setup. The results show a high consistency between the simulation and the experiment.

**Index Terms:** Waveguides, diffraction and gratings, heads-up displays.

## 1. Introduction

Holographic volume gratings (HVG) have been widely used in various optical applications because of the distinctive diffractive properties [1], [2]. Recently, the application of HVG as the couplers in a waveguide-based display system receives lots of attentions. Such a display system includes at least two holographic gratings as the in-coupling and the out-coupling gratings. The in-coupling grating is used to couple the light from the display panel into the waveguide system and the out-coupling grating is used to couple the propagating light out of the waveguide and send the images to the human eyes. In design, the diffractive efficiency (DE) of in-coupling grating is usually as high as possible to make sure the image brightness and the display light efficiency. Compared to the conventional grating, the HVG is capable of diffracting the light with the efficiency higher than 90% [3], [4], which makes the HVG become the promising candidate for the coupler for such a waveguide system. However, for the out-coupling grating the required DE different from and more complicated than that of the in-coupling grating. More specific, the required DE for an out-coupling grating is not a constant and but should vary in different exit pupil positions to guarantee the large exit pupil size and uniform image perception. As reported in [5]–[7], the diffractive efficiency should

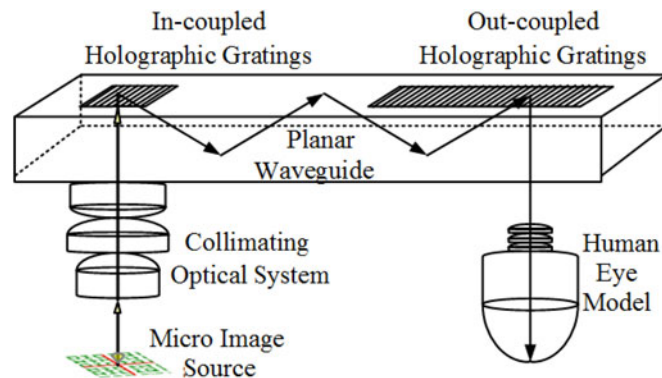


Fig. 1. Structure of a waveguide display system.

be a function of spatial position in the whole exit pupil. Ref. [8] proposed a distribution of diffractive efficiency for the out-coupling grating and the simulated results showed that the uniformity of output is increased effectively. However, most of previous researches considered the brightness uniformity only at the central view angle. However, in a real display application, a certain range of field-of-view (FOV) should be considered. These proposed DE distribution only can guarantee the uniform output for the central view angle, but for other view angles in FOV, the uniformity was not discussed. A more rigorous model should be built to simulate the waveguide system and investigate the optimal solution of DE distribution with considering the whole view angles in FOV. Meanwhile, the fabrication methods for such HVGs with the complex DE spatial distribution also need to be figured out.

In this paper, we build a more comprehensive physical model with considering the whole view angles in a relatively large FOV based on the ray tracing method. We propose an algorithm to derive a new DE spatial distribution for the out-coupling gratings, which can obtain a uniform output for a certain range of view angles in FOV. We also report the fabrication method of the HVG with proposed DE distribution to verify our algorithm by using the spatial light modulator (SLM) and holographic exposure setup. The results show a high consistency between the simulations and experiment, and a more uniform output in designed FOV can be achieved.

## 2. System Structure and Exit Pupil Expansion

A typical structure of the planar waveguide display system with holographic gratings is illustrated in Fig. 1 [9], [10]. The light from the micro display impinges the in-coupling grating after collimating by a collimating system with a 25 mm focal length, and diffracted by the in-coupling grating with angles satisfied the condition of TIR (Total Internal Reflection) and propagates along the waveguide. The out-coupling grating which is mirror symmetry as the in-coupling grating diffracts the light again and breaks the condition of TIR. This display system gives the output as the collimated light to the viewer, as a result the viewer can see a virtual image focused in infinity.

In Fig. 1, only the central view angle is illustrated. In practice, the light propagating in the waveguide can be depicted as Fig. 2. We assume the FOV is  $2\theta$  and the incident angles are range from  $-\theta$  to  $\theta$ . To simplify the analysis without losing its generality, only the margin incident angle  $\theta$  is discussed. After being diffracted by the input-coupling grating, the light propagates in the waveguide at angle  $\beta$ . The propagation period  $P$  can be determined by the waveguide thickness  $t$  and the beam propagating angle  $\beta$ , and the relation is  $P(\beta, t) = 2t \cdot \tan(\beta)$ .

Focusing on the principle of the exit pupil expansion, the out-coupling grating diffracts the light out of the waveguide as well as leaving a part of energy to propagate forward continuously. As a result, the light can be diffracted out of the waveguide in different positions. To uniform the output intensity, the DE of out-coupling gratings should be designed various along the waveguide. As illustrated as

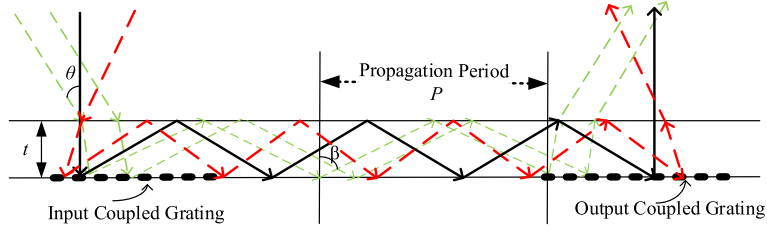


Fig. 2. Light propagation in the waveguide.

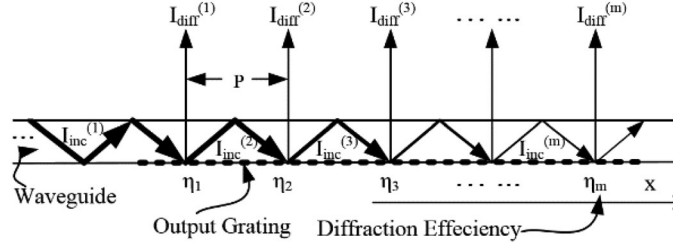


Fig. 3. Diffraction efficiency distribution sketch for the output coupling.

Fig. 3, by controlling the efficiency  $\eta_m$  along the propagating direction, the output intensity  $I_{diff}^{(m)}$  in different positions can be equal [11].

In Fig. 3 only the central view angle is considered. For the case of a relatively large FOV, different FOV angles corresponding to different propagation angles  $\beta_n$ . The beams propagating in the waveguide will be difference between the extreme angles of the entire FOV. Consequently, we have to resort to a numerical optimization method to satisfy uniformity of the relatively large FOV. In this procedure, as a criterion for the optimization, we minimize the integral deviation of the light diffracted out with different propagation angles. For  $N$  different propagation angles  $\{\beta_n\}_{n=1}^N$ , we chose coefficient of variation (C.V) of the light beams as the criterion:

$$C.V = \sum_{n=1}^N \left[ \frac{1}{\bar{I}_{diff}^{(\beta_n)}} \sqrt{\frac{1}{M} \sum_{m=1}^M (I_{diff}^{(m, \beta_n)} - \bar{I}_{diff}^{(\beta_n)})^2} \right] \rightarrow \min. \quad (1)$$

Where  $\bar{I}_{diff}^{(\beta_n)}$  denotes the mean intensity of the light diffracted out along the whole output grating with the specific propagation angles  $\{\beta_n\}_{n=1}^N$ , and  $m$  is the diffraction bounce number of each propagation angle.

$$I_{diff}^{(m+1, \beta_n)} = I_{inc}^{(m+1, \beta_n)} \bar{\eta}_{(m+1)} = I_{inc}^{(m, \beta_n)} (1 - \bar{\eta}_{(m)}) \bar{\eta}_{(m+1)} = \frac{I_{diff}^{(m, \beta_n)}}{\bar{\eta}_{(m)}} (1 - \bar{\eta}_{(m)}) \bar{\eta}_{(m+1)}. \quad (2)$$

We divide the output grating into  $K$  regions equally along the propagating direction,  $\eta_k$  is the efficiency of the  $k_{th}$  region ( $k = 1 \dots K$ ), the bigger  $K$  be chose, the more accuracy efficiency distribution will be calculated. According to a light beam's propagation cycle of the beams travelling inside the waveguide,  $\bar{\eta}_{(m)}$  is the local area's average efficiency of the  $m_{th}$  cycle covered. Here  $m$  stands for the bounce of the light beams propagating in the waveguide, the average efficiency is calculated from the weighted average of the corresponding covered regions' efficiency values  $\eta_k$  ( $k = m_1, m_2 \dots$ ). Different propagation period corresponding to the different covered regional, when taking enough  $\{\beta_n\}_{n=1}^N$  into calculation, we can get enough equation to derive out the most optimized DE distribution  $\eta_1 \sim \eta_K$  to satisfy the equation (1).

Usually, the HVG has a small bandwidth, and the diffraction efficiency of a HVG is heavily affected by the angle of incidence. For obtaining a large angular bandwidth to meet the actual needs of a

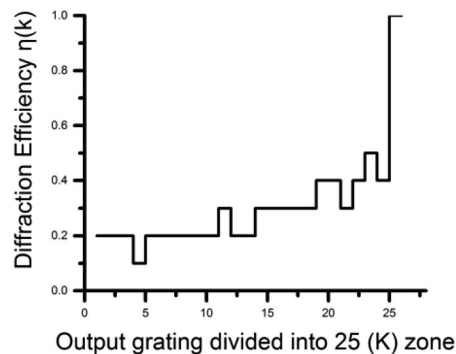


Fig. 4. The optimized diffraction efficiency distribution  $\eta(k)$  for the output coupling grating.

near-eye display system, it is necessary to use compound grating or multilayer grating, and even optimize the material of the holographic film to realize the big angular bandwidth [11], [12]. For simplicity, the means to meet the consistency of the efficiency within the larger angular bandwidth will not be described in this article.

The optimization algorithm is programmed by Matlab, which using an iterate procedure to search the appropriate value group of  $\eta_1 \sim \eta_K$  for getting the smallest C.V. In the process of iterations, in order to prevent C.V from converging to a local minimum, random scrambling has been carried out to ensure the robustness of the algorithm.

### 3. Program and Simulation

As an example, we investigate output gratings having lateral dimensions of 25 mm, the light beams' width  $W_{in}$  is 6 mm, the waveguide refractive index is 1.655, thickness is 2.5 mm. We set the required FOV as  $\pm 15^\circ$  in the air, for an appropriate grating period for the 532 nm wavelength, we can get the propagation angles  $\beta_n$  ranged from  $40^\circ$  to  $60^\circ$  [13]. For the optimization, 200 beams with the interval of  $0.1^\circ$  between  $40^\circ$  to  $60^\circ$  are set as propagation angles group  $\{\beta_n\}_{n=1}^N$ . The output grating is divided into  $K$  equilateral zones. Theoretically, selecting the bigger  $K$ , we can get the higher accuracy of the efficiency distribution, but the computational time consumed by the algorithm is greater. In the other hand, the size of the human eye pupil is  $3 \sim 7$  mm, taking into account the integral characteristics of the human eye, while the output grating's length is 25 mm, choosing  $K$  equal 25 is big enough for the accuracy.

The diffraction efficiency distribution  $\eta_k$  derived out by the program is showed in the Fig. 4. As shown, due to the consideration of large FOV, the optimized efficiency distribution curve is not monotonously increasing, which brings more precise requirements to the producing of the grating.

The C.V of the program criterion process is shown in the Fig. 5. If we choose the step efficiency distribution [14] as the initial efficiency distribution of the criterion, it showed that the C.V is 43% in our example. When the optimization program is executed, the C.V quickly converges to 29%. It means that the output uniformity of the waveguide display output is optimized nearly 14%.

When using the optimal DE distribution as Fig. 4, the output light intensity as a function of location along the output grating and the propagation angle are given in Fig. 6. The difference of the output light intensity in the entire FOV is lower than 0.3, while the input light beam's intensity is 1. As shown, it appears that the intensity at different angle is discrete. It means the different angle's light beams propagating in waveguide has different bounce distance. So we trace the propagating path of the light beams with the discrete angle individually, at last sample enough output beams with different angle altogether to derive out the optimal DE distribution. The optimal result is still discrete means that the propagation angle has main effect on the uniform of output intensity, while the sampling propagation angle is discrete in the simulation model.

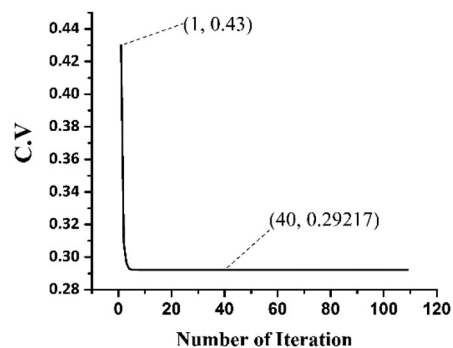


Fig. 5. C.V optimization process of the criterion program.

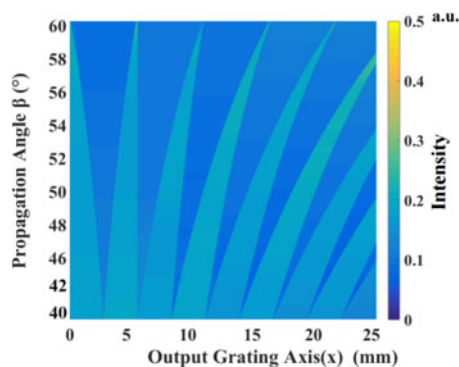


Fig. 6. Output light intensity as a function of location and propagation angle.

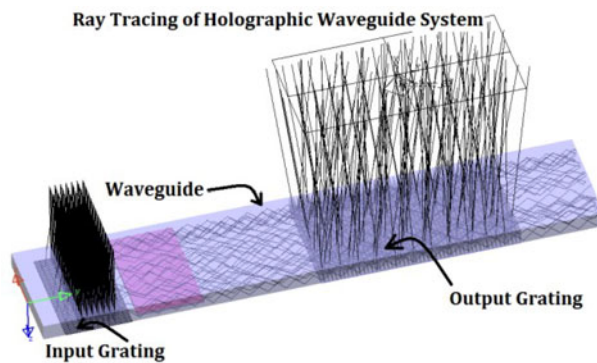


Fig. 7. 3D module and the ray tracing sketch for the holographic waveguide display system.

For simulating the output luminance of holographic grating display system with optimal DE distribution, we built the 3D module of the waveguide display system as shown in Fig. 7. Monte Carlo method is used for tracing the light ray propagating between  $40^\circ \sim 60^\circ$  in the waveguide. The luminance of light diffracting out from the out-coupling grating is shown in Fig. 8. From that we can see, the irradiance of output grating is fairly uniform for longer than 25 mm length.

#### 4. Experiment and Results

The schematic view of the optical system for fabricating the holographic grating with proposed DE distribution is shown in Fig. 9. The object light wave beam is turned  $90^\circ$  by a polarization beam splitter (PBS), and illuminates the reflective spatial light modulator (SLM). After modulating the

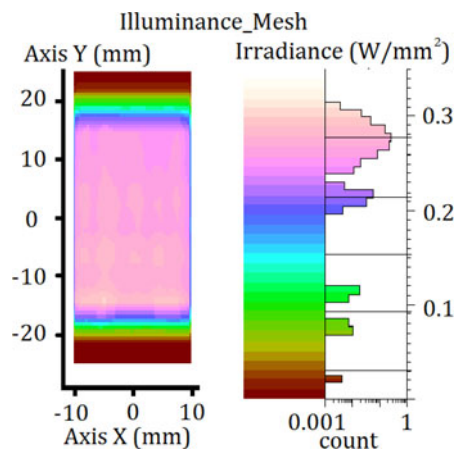


Fig. 8. Simulation results for the irradiance of output coupling grating.

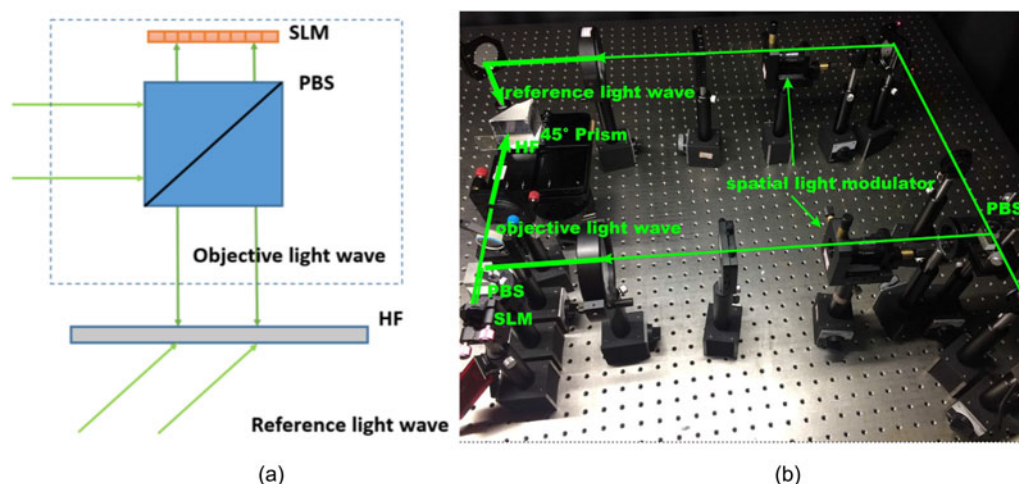


Fig. 9. (a) Schematic of the interferometric system. (b) Picture of the interferometric system: SLM—spatial light modulators, PBS—polarization beam splitter, HF—hologram film.

SLM, the desired light intensity distribution is formed and incident on the holographic film (HF). The reference light wave with uniform intensity incident on the film directly and overlapped with the modulated object light. By carefully controlling the exposure time and the ratio of the object light intensity to the reference light intensity, the holographic grating with variable diffractive efficiency can be recorded in the film.

From the basic principle of the holographic technology, the desired interferometer fringe  $I(x, y)$  can be described as

$$I(x, y) \propto \langle O(x, y)R^*(x, y) \rangle. \quad (3)$$

Where  $O(x, y)$  and  $R(x, y)$  are the complex amplitudes of the object light wave and the reference light wave, respectively. The superscription '\*' means the conjugation, and  $\langle \dots \rangle$  denotes the time average. Normally,  $R(x, y)$  is assumed as the plane wave that can be constructed simply in the experiments. How to determine the complex optical field distribution of  $O(x, y)$  is a key to obtain the desired fringes. The solution to obtain the target optical field distribution is shown in Fig. 9. The mechanism of interferometer is employed to achieve the object light wave, where a coherent parallel light beam is modulated by a SLM, and then project to the exposure film.

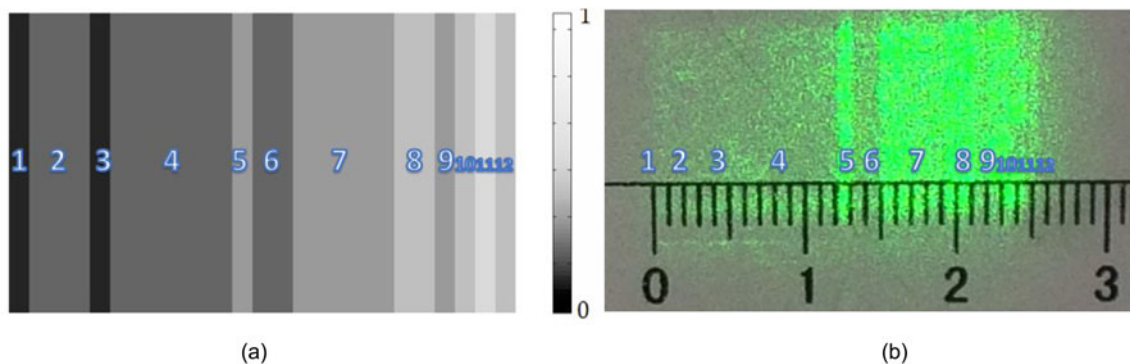


Fig. 10. (a) Input gray level distribution for the SLM. (b) Output light intensity distribution for the SLM gray map (a) as the input of the SLM and (b) the output of the SLM.

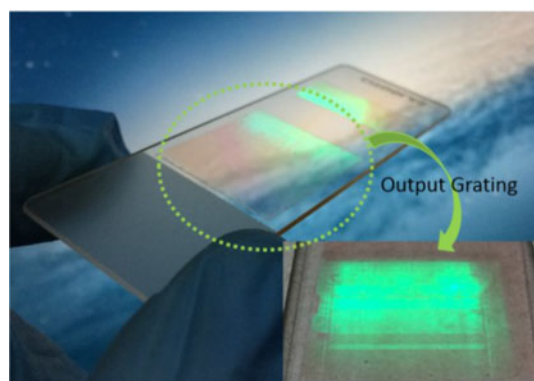


Fig. 11. The fabricated holography grating stamp on the waveguide and the light distribution diffracted from the output coupling grating.

According to coupled-wave theory, the diffraction efficiency for a slanted reflective linear grating without absorption [15], [16] (the photopolymers we used here have high transparency after recording and UV flood cure, and the test absorption rate is less than 2% at 532 nm wavelength. For simplify, the effects of material absorption are temporarily ignored in this analysis) in Bragg angle can be written in the form

$$\eta = th^2 \left( \frac{\pi \Delta n d}{\lambda (\cos \theta_r \cos \theta_s)^{\frac{1}{2}}} \right). \quad (4)$$

Where  $\Delta n$  is the modulation of the refractive index,  $d$  is the thickness of the recording material,  $\lambda$  is the reconstruction wavelength, and the  $\theta_r$ ,  $\theta_s$  are the obliquity angle of the readout and diffracted beams in the recording medium, respectively. It can be assumed that the fabrication of the holographic grating satisfied the linear recording condition, so the fringe intensity distribution of the light can be inverted into the modulation of the refractive index distribution linearly [15], [16].

The input image of the SLM is showed in Fig. 10(a), which is converted from the optimized curve in Fig. 4. The output modulated image is showed in Fig. 10(b) which contains 12 areas with different intensities. By setting the total exposure power to be 15 mW/cm<sup>2</sup>, the reference and the object light's ratio to be 1:1.75, the exposure time to be 25 s, the holographic grating with desired DE distribution is recorded on the hologram film. In a specific angle, we can see the corresponding efficiency changes of the output grating showed in Fig. 11. The thickness of photopolymer



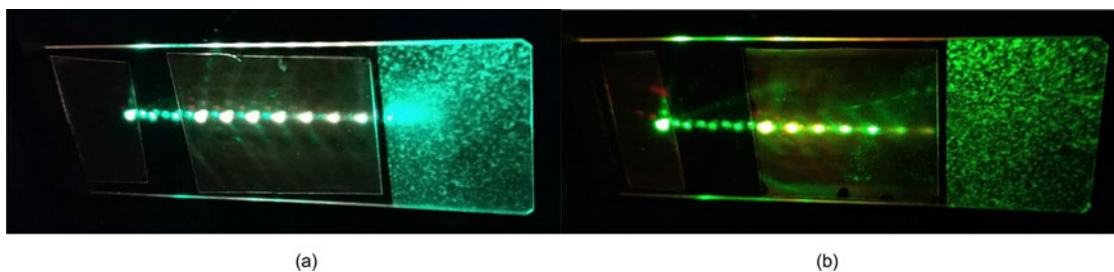


Fig. 12. Laser beam propagating in waveguide when the output grating (a) with efficiency optimization and (b) without efficiency optimization.

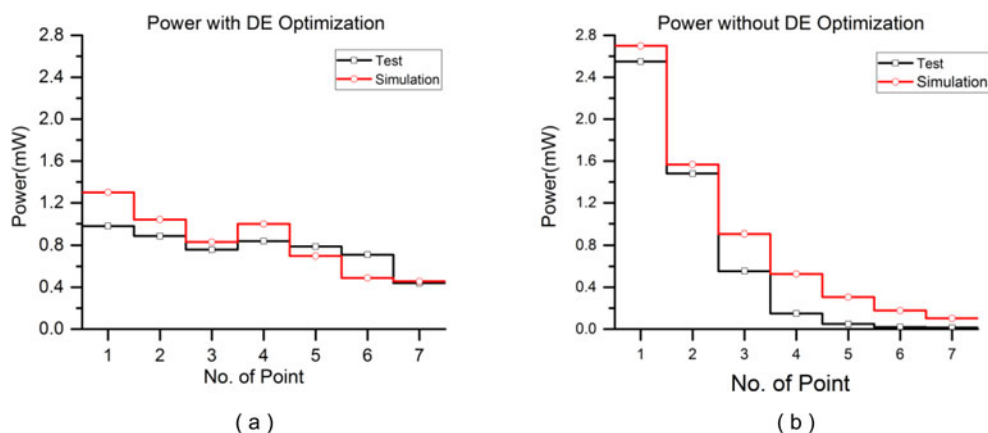


Fig. 13. (a) Test power of 7 output light beams with efficiency optimization grating. (b) Test power of 7 output light beams without efficiency optimization grating.

layer is 16  $\mu\text{m}$ , the maximum refractive index modulation  $\Delta n$  is bigger than 0.08 theoretically. The grating period of the gratings we recorded is 177 nm, and the in-coupling grating's Bragg angle at normal incidence is  $26^\circ$ , and the out-coupling gratings' Bragg angle at normal incidence is  $-26^\circ$ .

Fig. 12 shows the comparison of the output between the out-coupling grating with proposed DE distribution and the constant DE. As shown in Fig. 12(a), the output intensity is more uniform in out-coupling with proposed DE distribution compared with the out-coupling with constant DE (Fig. 12(b)), and the light can propagate with a longer distance because of the designed DE distribution. In the test, the input laser beam's power is 10 mW, and the corresponding output beam's power of each point is shown in Fig. 13(a) and (b). As well, the simulation of the output power is shown in Fig. 13(a) and (b), the uniformity and the trend of the output's power in the simulation and test results are almost the same. The difference comes from the DE consistency between the real gratings and the designed ones. And the simulation of overall efficiency of the two output grating is 77% and 79% respectively. From that we can see, the overall efficiency is compromised but acceptable when optimizing for output uniformity.

When assembling the designed holographic waveguide with the appropriate micro-display system (as shown in Fig. 1), we can get a planar display system. The actual display performance of demonstrated holographic waveguide display system is showed in Fig. 14. Furthermore, to evaluate the uniformity of the output in whole FOV ( $30^\circ$ ), we set a uniform green picture as the input of the waveguide display system, and use the CS-200 Luminance and Color Meter to test the luminance of five points (as shown in Fig. 15) in the output region. The test results are showed in Table 1, the output luminance of 3 representative angle at the different point of the

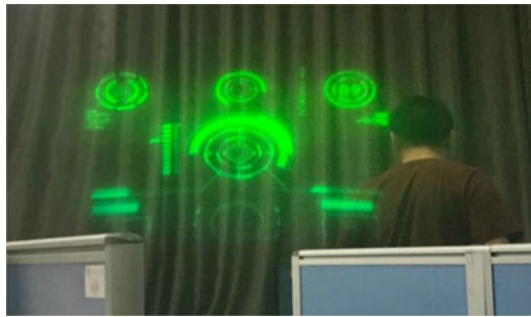


Fig. 14. The actual effect of holography waveguide display system.

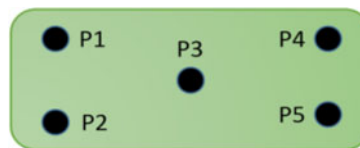


Fig. 15. Five test points selected on output grating.

TABLE 1  
The Luminance of the Output

| Luminance(cd/m <sup>2</sup> ) | Point 1 | Point 2 | Point 3 | Point 4 | Point 5 |
|-------------------------------|---------|---------|---------|---------|---------|
| Left edge of FOV              | 100.56  | 100.78  | 92.27   | 66.21   | 33.92   |
| center of FOV                 | 113.59  | 101.88  | 97.08   | 74.24   | 55.3    |
| right edge of FOV             | 100.93  | 93.24   | 92.83   | 65.24   | 39.71   |
| C.V                           | 0.2897  |         |         |         |         |

output grating are relative uniform. Meanwhile, the C.V of these test points are matched with the simulation well.

## 5. Conclusion

Considering the uniformity of the waveguide display's output with a 30° FOV, it is necessary to model the planar waveguide display system carefully, and optimize the output grating efficiency distribution. In experiments, a spatial light modulator (SLM) is applied as the spatial luminance modulator, and the coupling grating with proposed DE distribution is fabricated by the holographic interference exposure setup. The result shows the proposed DE distribution works well at the uniformity of the entire FOV.

## References

- [1] R. P. G. Collinson *et al.*, *Introduction to Avionics Systems*. New York, NY, USA: Springer, 2011.
- [2] L. Ao *et al.*, "Realization and optimization of holographic waveguide display system," *Acta Optica Sin.*, vol. 37, no. 5, 2017, Art. no. 0523003.
- [3] R. Shechter, Y. Amitai, and A. Friesem, "Compact beam expander with linear gratings," *Appl. Opt.*, vol. 41, no. 7, pp. 1236–1240, 2002.
- [4] R. Shechter, Y. Amitai, A. A. Friesem, and S. Reinhorn, "Planar holographic configuration for efficient imaging," *Opt. Commun.*, vol. 132, pp. 221–226, 1996.
- [5] Y. Amitai, S. Reinhorn, and A. A. Friesem, "Visor-display design based on planar holographic optics," *Appl. Opt.*, vol. 34, no. 8, pp. 1352–1356, Mar. 1995.
- [6] A. S. Maimone, "Computational see-through near-eye displays," Ph.D. dissertation, Univ. North Carolina Chapel Hill, Chapel Hill, NC, USA, 2015.

- [7] I. Gurwich *et al.*, "Design and experiments of planar optical light guides for virtual image displays," *Proc. SPIE*, vol. 5182, pp. 212–221, 2003.
- [8] R. Shechter, S. Reinhorn, Y. Amitai, and A. A. Friesem, "Planar holographic elements with uniform diffraction efficiency," *Appl. Surf. Sci.*, vol. 106, pp. 369–373, 1996.
- [9] J.-W. Pan and H.-C. Hung, "Optical design of a compact see-through head-mounted display with light guide plate," *J. Display Technol.*, vol. 11, no. 3, pp. 223–228, Mar. 2015.
- [10] I. A. Baker and V. A. Handerek, "Waveguide," U.S. Patent Appl. 20110026128A1, Feb. 3, 2011.
- [11] Z. Shen, Y. Zhang, Y. Weng, and X. Li, "Characterization and optimization of field of view in a holographic waveguide display," *IEEE Photon. J.*, vol. 9, no. 6, Dec. 2017, Art. no. 7000911.
- [12] T. Levola, "Diffractive optics for virtual reality displays," *J. Soc. Inf. Display*, vol. 14, pp. 467–475, 2006.
- [13] L. Eisen *et al.*, "Planar configuration for image projection," *Appl. Opt.*, vol. 45, no. 17, pp. 4005–4011, 2006.
- [14] Z. Wu, J. Liu, R. Shi, and Y. Wang, "The recording method of planar holographic grating with variable diffraction efficiency by phase modulations," *Opt. Commun.*, vol. 298–299, pp. 41–45, 2013.
- [15] H. Kogelnik, "Coupled wave theory for thick hologram gratings," *Bell Syst. Tech. J.*, vol. 48, pp. 2909–2947, Nov. 1969.
- [16] M. G. Moharam and T. K. Gaylord, "Rigorous coupled-wave analysis of planar-grating diffraction," *J. Opt. Soc. Amer.*, vol. 71, pp. 811–818, 1981.